EJONS International Journal on Mathematic, Engineering and Natural Sciences ISSN 2602 - 4136

Article Arrival Date	Article Type	Article Published Date
1.09.2020	Research Article	15.12.2020

Doi Number: Doi Number :http://dx.doi.org/10.38063/ejons.333

INVESTIGATION, MODELING, AND SIMULATION OF RADIOFREQUENCY ABLATION SYSTEMS WITH FINITE ELEMENT METHOD FOR VARICOSE VEIN TREATMENT

Batur Alp AKGÜL*
Hasan Kalyoncu University, Institute of Science, Electrical & Electronics Engineering, Gaziantep, TURKEY, baturalpakgul@gmail.com, ORCID: 0000-0002-8332-6764.

Ercument KARAPINAR
Hasan Kalyoncu University, Engineering Faculty, Electrical and Electronics Engineering, Gaziantep, TURKEY, ercument.karapinar@hku.edu.tr, ORCID: 0000-0002-9328-1969.

ABSTRACT

The modern thermal method of a treatment process for varicose veins (VV) is radiofrequency ablation (RFA) which is extremely prevalent. VV impairs quality of life, and RFA may be used to treat VV. This technology has been used widely recently for treating VV. The finite element method (FEM) plays an important role in performing interactive simulations of biological systems. FEM requires complex geometries to be computed that cannot be solved by analytical techniques. Therefore, Bio-Heat equations are formulated and used based on FEM. It is very suitable for the efficient simulation of RFA operations. This paper presents the investigation and simulation of RFA using the application of FEM Multiphysics regarding the flow of the blood and vein wall for VV treatment accordingly. In this study, a model has been constructed to measure and evaluate the effects of RFA for the vein wall and the blood, and a computer-based simulation is performed to calculate the influence of heat generated from the RFA device on the blood flow. For an effective analysis, a simplified 3D vein geometry is used to measure temperature profiles in the vessel wall and to analyze the thermal properties of flowing blood. Obtained numerical results and simulations can be used as an asset in future studies.

Keywords: RFA, VV, FEM, Temperature, Blood, Heat, Simulation.

1. INTRODUCTION

VV is considered to be a severe chronic venous insufficiency, and RFA is used to kill or eliminate infected varicosity veins. RFA is the removal or destruction of a vein segment using RF energy. As they are minimally invasive, it is developed as alternatives to surgery. RFA is a VV treatment involving the delivery of controlled RF energy through a catheter inserted into the affected vein where the electrical conduction system destroys or treats the tissue by heating the target domain with RF energy [1]. During the RFA process, under imaging guidance, a catheter electrode is inserted into the target domain of the damaged tissue. Another electrode is placed outside the body that closes the catheter and is heated by electric RF. One of the main goals of RFA is to disrupt and destroy abnormal pathways that contribute to varicose veins. This research focused on using RFA only in VV treatment, and research was carried out in this direction. So, the purpose of this study is to present modeling and simulation for the treatment of VV using RFA. One of the other goals of this study is to present the effects of the electrode-generated RF heat on the vein wall of the blood and varicose veins. Realized RFA computer simulation is carried out to measure the impact of the heat produced from the electrode and compute the venous wall temperature profiles.

2. LITERATURE REVIEW AND RELATED WORKS

Several studies on the modeling of RFA systems are available in the literature. RFA is a procedure where part of the damaged tissue is ablated using the heat produced from RF [2-3] current alternating. The key advantage of the RF current is that it does not interfere with the bio-electric signals. Significant advantages in the last few years have contributed to the widespread use of RFA [4-5]. RFA is today a highly safe and effective technique for varicose vein management [6]. Mathematical modeling performed a simulation of thermal effects in various RFA applications for VV. Computer models for RFA have developed to measure the scope of the lesion with a thermal damage function [7–8]. The impacts of the tissue-electrode angle on temperature and blood flow distribution with current density distribution during RFA were studied in [9].

3. BACKGROUND AND BASIC PRINCIPLES OF THE RFA

RFA operates between 375–550 kHz frequencies. The electrical current is applied to the ablation domain by using an active probe. During the interval of 4–6 minutes [10], the electric current flow transfers the energy to the tissue that produces a temperature of up to $100°C$. Electrical current flowing through the tissue and causing volumetric heat generation as well as heat exchange in thermally conductive tissues are the basic physical processes that occur during RFA [11].

RF is a source of electromagnetic energy, and the RFA signal generator is an essential part of the RFA system. Energy stored by the electrode is produced here. The machine consists of a circuit for the RF generator, a circuit for the RF power amplifier, and the control circuit. Also, included is a power supply circuit for satisfying the system's power supply requirements. The active electrode provides the tissue with the power produced by the device. whereas a dispersive electrode provides a return part for the completion of the circuit. Figure 1 represents an RFA block diagram.

RFA 's purpose is to therapy thermal tissue injury by usage of electrical energy. RFA is physically dependent on the RF current of approximate value 460kHz (375kHz-550kHz) passing from the tip of a thermal RF sample to a dispersive electrode that acts as a grounding surface through the target tissue. The two electrodes are connected to a generator of RFs. The active electrode has a very small cross-sectional area according to the passive electrode. Depending on the joule effect, the tissue near the electrode is hot, and the temperature in areas remote from the electrode increases with thermal conduction. Thermal damage caused by RF heating can be varied depending on both the tissue temperature obtained and the heating time. Also, knowing the temperature allows correcting for variable speeds. The RFA scheme diagram is shown in Figure 2.

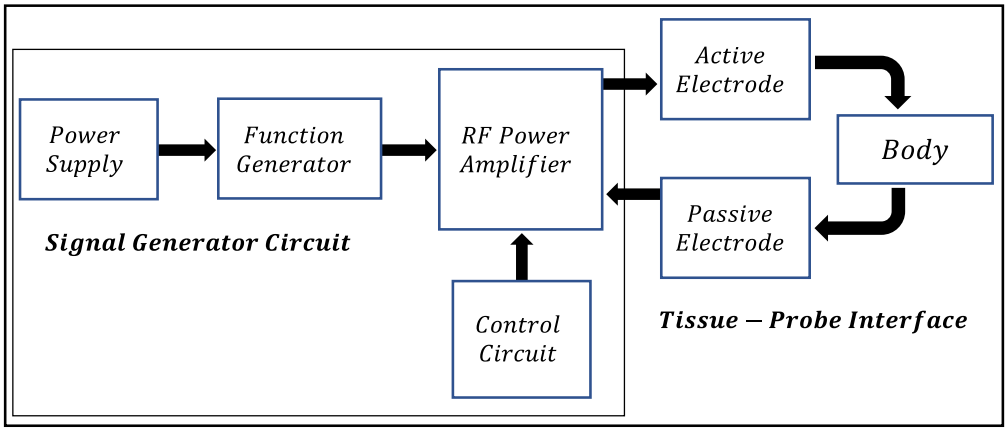

Figure 1: Block diagram of the RFA circuit

The tissue temperature should be kept in the optimal range to ensure efficiently ablate the VV, to prevent carbonization around the edge of the electrode because of the heating unnecessarily [12], and to induce tissue death in the ideal value of 50°C-100°C. One of the key principles of RFA is

therefore to obtain and sustain a temperature value of $50°C - 100°C$ for at least 4 – 6 minutes over the entire target volume [13]. Additionally, the slow thermal conduction from the electrode to the surface through the tissue can be increased the application duration to 10-30 minutes.

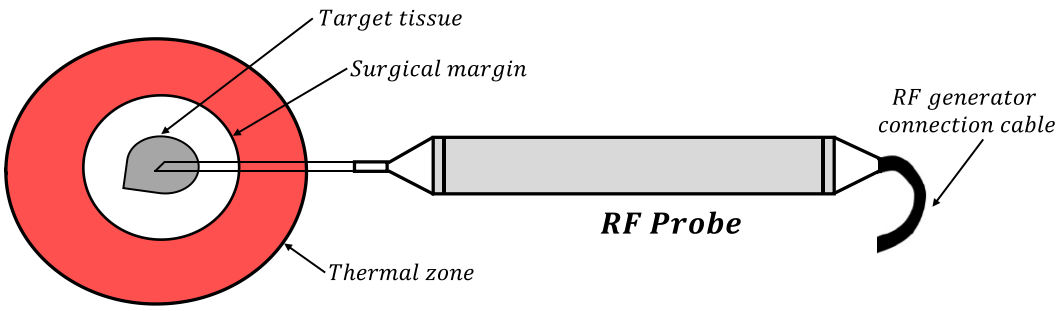

Figure 2: Schematic diagram of the RF Probe

The area heated by the RFA probe more than $50°C$ is irreversibly degraded or changed. Therefore, the RFA must be conducted in one volume and part by part restricted to the intended VV domain so that unintended damage to the tissue is prevented. To prevent micro-burns in VV tissue, it is necessary not to exceed $100°C$ to control the temperature of the VV domain. Thus, it is important to research and examine whether the current temperature and density are spread around the ablation electrodes. Precise temperature measurement is critical for the prediction of unwanted damage in an ablation phase. To prevent unwanted damage and keep RFA processes under control, the temperature of the tissue should be monitored precisely. Thus, in this analysis, the numerical bio-structural model has been used, and the relationship between RF source and VV tissue has been examined [14-15].

4. FEM-BASED NUMERICAL MODELING

The bio-heat equation is so-called Penne's Formula, and it is mainly used to formula the electrical–thermal heating cycle. The formula executes the increasing temperature at any point in the VV domain during the RFA [16-17]. The RFA probes operates between 460kHz-550kHz. The magnitude of electromagnetic energy at these frequencies is larger than that of the RFA energy of the electrodes. Therefore, the primary mode of transmission of energy is through electrical conduction. It can be modeled as quasi-static electrical conduction and heat conduction based on FEM with the continuity and the momentum function equations. These equations are given by (1) and (2).

$$\rho c \frac{\partial T}{\partial t} = \nabla . k \nabla T + JE - h_{bl}(T - T_{bl}) - Q_{el} \quad (1)$$

$$(h_{bl} = \rho_{bl} c_{bl} w_{bl}) \quad (2)$$

Where,
ρ is the density of the mass, c is the capacity of the heat, k is the thermal conductivity, J is the density of the current, E is the intensity of the electric field, ρ_{bl} is the density of the blood, C_{bl} is the heat capacity of the blood, W_{bl} is the perfusion rate of the blood, T_{bl} is the temperature of the blood, Q_{el} is the heat exchanged between the RFA electrode and the tissue.

The blood flow is a part of the bio-heat governing equations in FEM-based modeling. Based on the blood parameters used in the bio-heat and conduction models, blood flow can be varied. The bio-heat equations are indicated the heat transfer with blood flow and the diffusion of heat in the blood. Moreover, the blood viscosity is computed as Newtonian fluid [18-19] and it is expressed with the Carreau-Yasuda model using equation (3).

$$\frac{\mu-\mu_\infty}{\mu_0-\mu_\infty} = [1 + (\lambda\acute{y})^a]^{(n-1)/a} \quad (3)$$

Where,
μ_∞ is the viscosity at an infinite shear rate, μ_0 is the viscosity at zero shear rate, λ is the relaxation time, n, a are the non-dimensional power indexes, $\acute{y}$ is the shear rate for shearing deformation is applied to blood.

5. FEM-BASED IMPLEMENTATION

This section describes the application of the proposed numerical model using physical geometry in figure 3 and figure 4. The implementation of the numerical model is performed using the FEM. The model is performed in a computational environment for FEM with CFX Fluid Flow Module that is consist of FEM volume codes where the flow equations are discretized for each cell in the FEM software. Used parameters and boundary conditions in the FEM simulations are given in table 1.

Table 1: The used parameters in the FEM simulations

Symbol	Description	Value
P_{vv-bl}	Blood Density	$1050 kg/m^3$
μ_b	Blood Dynamic Viscosity	$0.0035\ kg/m^3$
P_{vv-wl}	Vein Wall Density	$1120\ kg/m^3$
C_{vv-bl}	Blood Heat Capacity	$3820\ J/kg°C$
C_{vv-pwl}	Vein Wall Heat Capacity	$3780\ J/kg°C$
K_{vv-bl}	Blood Thermal Conductivity	$0.492\ W/mK$
K_{vv-wl}	Vein Wall Thermal Conductivity	$0.56\ W/mK$

Source: [20-21], (2006, 2012).

It is assumed that the thermal boundary state has zero heat flux, and the electrode surfaces have source of heat to preserve constant temperature. The temperature transmitted from the heat source

can be entered into the interfacial plane and the energy flow can be carried out through the wall of the vein. The inlet blood temperature is assumed the same as human body temperature $(36°C)$, the heat flux is assumed as zero and is applied at the exit of the blood flow. It is assumed that the tissues with constant electrical and thermal conductivity can be regarded as a homogeneous medium. In other words, the vein wall is considered as homogeneous and isotropic. The blood flow at the inlet of the vein wall is considered as continuous laminar flow with a uniform velocity profile. Moreover, it is assumed that the blood flow is laminar due to the structure of varicose veins. The simulation environment has been prepared under these assumptions and the boundary conditions in table 1 have been used in the simulations.

Figure 3 shows the vein model schematics used for simulation. Where D represents the diameter of the vein $(2R)$ d represents the diameter of the electrode, L represents the length of the electrode, and t represents the thickness of the vein wall. The vein and electrode geometry are plotted in the radius of the vessel and tissue for the VV domain. In this sample, the VV domain is composed of the lumen and the vein wall. The lumen which means space in the vein is $4mm$ in diameter and $60mm$ in length. The thickness of the vein wall is $0.6mm$ in with the interface between the blood and the vein wall. It is the innermost of the three layers that make up the vessel wall, the inner layer of the blood vessel. The diameter of the electrode is in $0.5mm$, the length of the electrode is in $10mm$. The

electrode is in the middle of the lumen and 20 mm away from the inlet. The simple geometry in Figure 3 is represented by figure 4 depending on the mesh structure when drawn in 3D in the simulation environment.

The governing equations are solved using the FEM Multiphysics application where flow equations are discrete for each cell in the system and mesh structure is created by the FEM software. So, it is solved the governing equations with the RFA electrode properties to measure the flow of the blood and the distributions of the temperature in the VV domain. The properties of the materials and the values used in this study are shown in table 1, and detailed information about materials and values can be found in [21].

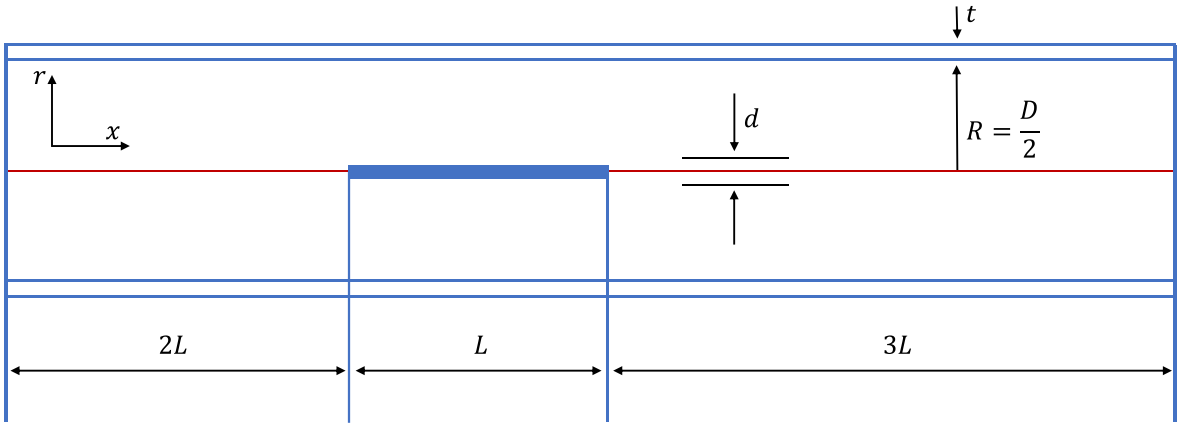

Figure 3: Schematic diagram of the model used for simulation

The FEM application used to support mesh partitioning and it has been used various surface mesh preparation instruments for the segmented venous wall in the FEM software to provide effective meshing. The FEM device surface mesh density helps us to conveniently use stages of surface preparation and volume estimation within device infrastructure. Typical surface mesh sizes are several hundred thousand triangular elements of the order of 1,6 million elements with resulting meshes in the volume. The size of the mesh depends partly on the vein size near the ablation site. The larger the size of the vein, the more complicated the meshing of the surface, and the greater the number of elements in the length mesh. In this study, the most appropriate and efficient mesh structure for VV treatment has been presented and calculations have been made with 4 processors in parallel processing mode.

6. RESULTS AND DISCUSSIONS

The half-vessel model, presented in a simple diagram in section 5.2, is drawn in 3D with the FEM software. Figure 4 shows the 3D vein model. The vein wall is given in figure 4(a), the RF-anode electrode placed in the vein wall is given in figure 4(b), and blood fluid with symmetry in the vein wall is given in figure 4(c). Arrow marks represent the direction of blood flow and they are called inlet and outlet. The temperature distribution of the VV domain is given in figure 5. It is seen that from figure 5, the blood temperature in the VV domain reaches $353\text{K}\,(79.85°\text{C})$ from $309\text{K}\,(35.85°\text{C})$ in 0.03 meters (it is default body temperature) with the heating of the RF electrode, and it appears that blood flow continues at $331\text{K}\,(57.85°\text{C})$ after a total of 0.06 meters. The maximum temperature value can be $373K\ (99.85°C)$ for the RF electrode and in this simulation, the value has been set to $353\text{K}\,(79.85°\text{C})$, if this value is exceeded, the tissues will be permanently damaged. Therefore, heat management is very essential in the RF electrode determined by VV ablation requirements.

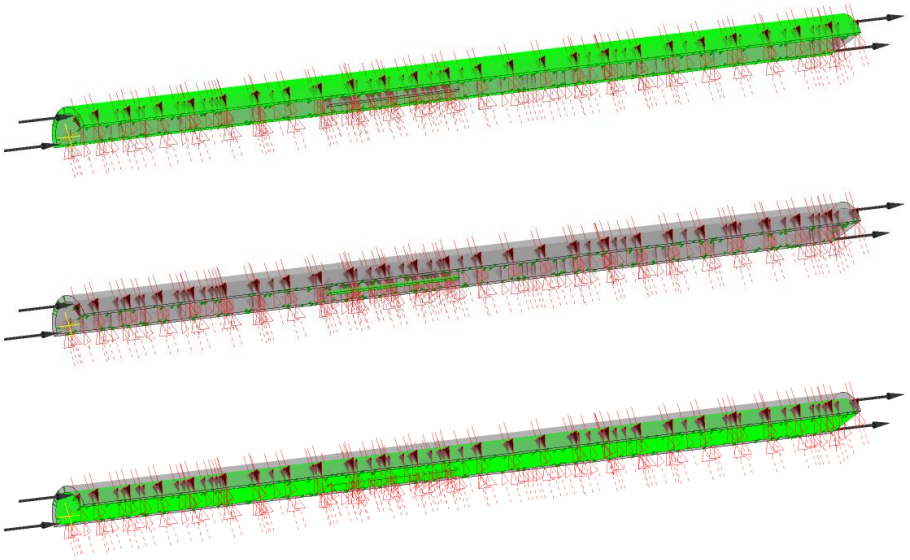

Figure 4: The 3D vein model presented in the FEM application

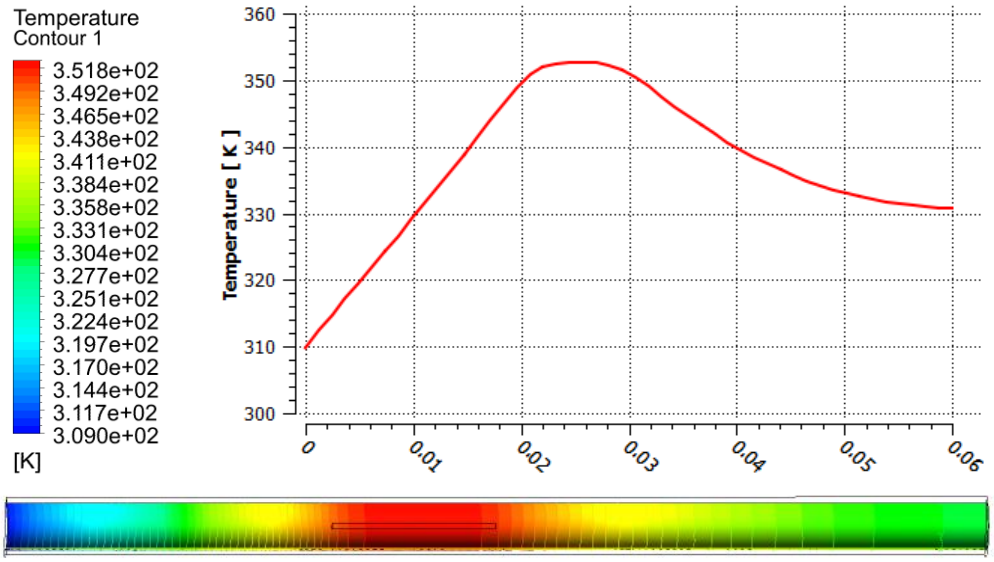

Figure 5: Temperature distribution of the VV domain

Figure 6(a) and figure 6(b) show the momentum and mass analyses for the RMS and the MAX residuals reached in the simulation during the blood flow in 30 seconds in the VV domain. It is observed that the root mean square (RMS) residuals and MAX residuals for $\mathrm{P, U, V, W}$ velocity components value are between $1X10^{-06}$ and $1X10^{-04}$ with meshed 1.6 million cells while the blood velocity is $10mm/s$. Additionally, Figure 6(c) and Figure 6(d) show that the heat transfer values for the RMS and the MAX residuals reached simulation during the blood flow in 30 seconds with $10mm/s$ velocity in the VV domain. It is seen that from the heat transfer analysis in figure 6, the RMS and the MAX residuals for H-Energy in the blood and T-Energy in the vein wall values are between $1X10^{-05}$ and $1X10^{-04}$ with meshed 1.6 million cells while the blood velocity is $10mm/s$.

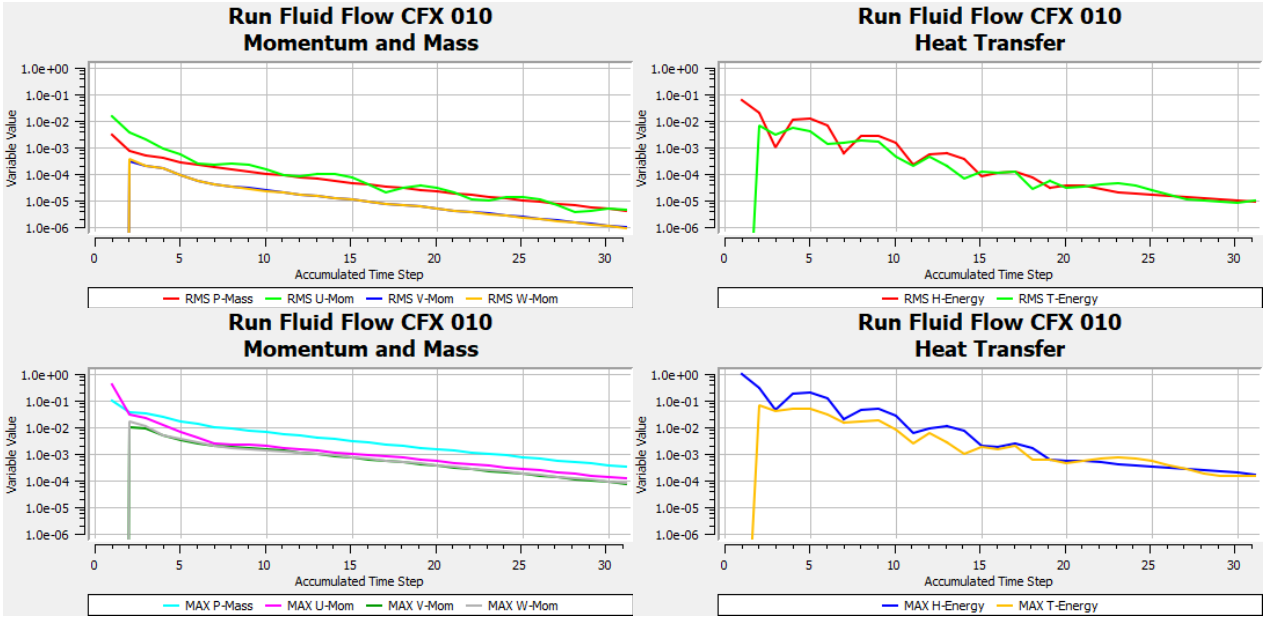

Figure 6: The momentum, the mass, and the heat transfer analyses for the RMS and the MAX 6(a): The momentum and the mass values for RMS, 6(b): The momentum and the mass values for MAX, 6(c): The heat transfer for RMS, 6(d): The heat transfer for MAX.

It is understood from the analysis results in figure 6, there is a compatibility between the designed numerical model and the FEM based simulation results. While blood velocity is flowing at a constant speed as $10mm/s$, the temperature increased by giving RF energy by anode interface has started to cool within a certain time in the VV domain. Then, (after the $25th$ second), the blood and vein wall appear to have reached an equal temperature value.

Active electrical conductivity dominates the RF electric current processes. In the VV tissues, the heat generation is determined by the density of the electrical current. At the same time, the conductivity of the VV tissue depends on the non-linear VV tissue temperature. The prepared numerical model provides an acceptable point of departure to simulate but does not show the entire image. The electric field not only functions for the boundary but also as a source term that supplies energy to the whole system.

Besides, the tissue's electrical conductivity behaves as a constant variable, but it is not constant, it is a variable depending on the temperature. Governing equations numerically solve that the temperature reaches the desired point in the entire VV tissue under the specified initial and boundary conditions, a constant electric field, and blood perfusion. For these reasons, to correct these issues and eliminate deficiencies, making special revisions in governing equations and designing a computer-based FEM application accordingly may be a more realistic approach and give more realistic results.

In Figure 7, the temperature distribution occurring in the blood with the effect of the RF anode electrode placed in the VV domain is shown in a symmetrical plane. While the temperature in the blood on the inlet side of the VV domain is $309\text{K}\,(35.85°\text{C})$ up to 25 millimeters, when $353\text{K}\,(79.85°\text{C})$ RF energy is transmitted to the blood by the active probe, a sudden increase in blood temperature occurs after 30 millimeters, and when it reaches 60 millimeters, the blood temperature reaches $314\text{K}\,(40.85°\text{C})$. During this measurement, blood velocity is 10mm/s. By increasing the temperature of the anode electrode up to $373K\ (99.85°C)$, the temperature change in the blood can be further increased in accordance with the requirement. It is possible to achieve more positive results in RFA treatment by controlling the heat energy in the blood.

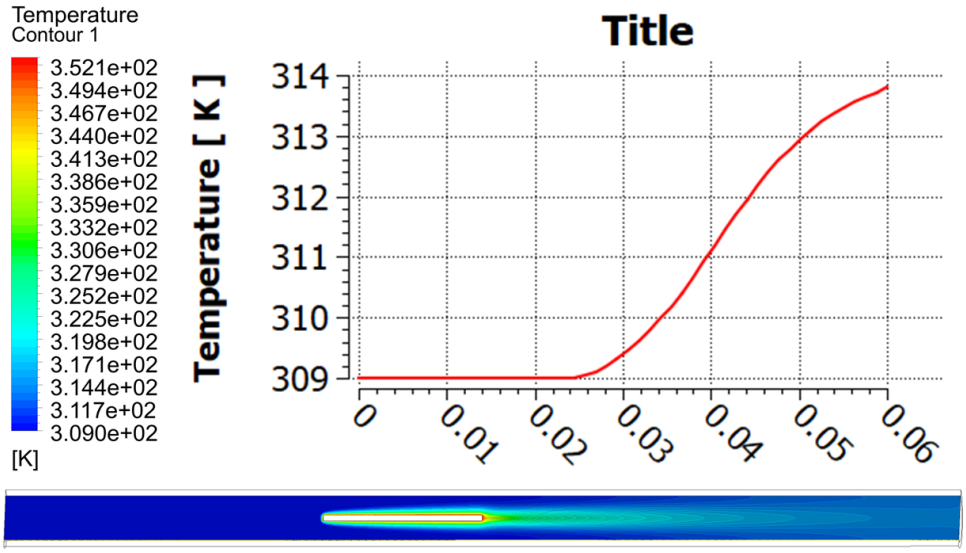

Figure 7: Temperature distribution of the VV domain on the symmetrical plane

7. CONCLUSIONS

The non-linear computational model for the VV domain and a FEM specialized for RFA has been presented. In this study for simulating the RFA processes and considering electrical and thermal events in the VV domain tests have been carried out on the physical properties of the thermal effects in the VV tissue and the findings evaluated. In this analysis, the FEM simulation is based on RFA's numerical model for VV, and the simulation is carried out using FEM Multiphysics tools. During the RFA simulation, differences in operating frequency temperatures of the VV tissue and input of the RF energy injected into the VV surface was measured.

It has been seen in the simulations, the size of the VV domain to be applied RFA, the boundary conditions, and parameters are very important for a successful treatment. As the VV region shrinks, it seems likely that the success rate in treatment will increase depending on the temperature and blood velocity. Therefore, RFA implementation in a small domain to be determined beforehand may be more successful.

In this study, a simplified heat conduction model with modified boundary conditions has been derived due to the non-linear nature of the vein tissue, electrical conductivity, and the complexity of the bio-heat equation. The FEM-based simulations for the VV domain were conducted on the RFA by using a temperature-dependent conductivity solution. Temperature distributions were measured using FEM software to see the effects of frequency, RF energy, probe depth inserted in the VV domain. Each one of these parameters plays an essential role in providing optimum thermal values for RFA therapy. Obtained results and simulations can be used as an asset in future studies.

REFERENCES

[1] Townsend, C., Beauchamp, R.D., Evers, B.M. & Mattox K. (2016). Sabiston textbook of surgery: the biological basis of modern surgical practice, PA: Elsevier Saunders, pp. 236.

[2] Quaranta V., Manenti, G., Bolacchi, F., Cossu, E., Pistolese, C.A. & Buonomo O.C. (2007). FEM Analysis of RF Breast Ablation: multiprobe versus Cool-tip Electrode, Anticancer Res, pp. 775–84.

[3] Tungjitkusolmun, S., Staelin, S.T., Haemmerich, D., Tsai, J.Z., Cao, H. & Webster, J.G. (2002). Three-dimensional finite-element analyses for radio-frequency hepatic tumor ablation, IEEE Trans Biomed Eng, pp. 3–9.

[4] Abdelalim, A., Ali, M.S. & Elgammal, A. (2013). Study of the efficacy of combined RF ablation and percutaneous acetic acid injection in the management of hepatocellular

carcinoma, pp, 31–39.
[5] Livraghi, T. (2003). Radiofrequency ablation, PEIT, and TACE for hepatocellular carcinoma, J Hepatobiliary Pancreat Sur, pp. 67–76.
[6] Dunn, C.W., Kabnick, L.S., Merchant, R.F., Owens, R. & Weiss, R.A. (2006). Endovascular radiofrequency obliteration for treatment of great saphenous vein, Annals of Vascular Surgery, pp. 625–629.
[7] Chang, I.A. & Nguyen, U.D. (2004). Thermal modeling of lesion growth with radiofrequency ablation devices, BioMedical Engineering Online, pp. 1-19.
[8] Jain, M.K. & Wolf, P.D. (2000). Three-dimensional finite element model of radiofrequency ablation with blood flow and its experimental validation, Annals of Biomedical Engineering, pp. 1075–1084.
[9] Panescu, D., Whayne, J.G., Fleischman, S.D., Mirotznik, M.S., Swanson, D.K. & Webster J.G. (1995). Three-dimensional finite element analysis of current density and temperature distributions during RFA, IEEE on Biomedical Engineering, pp. 879–890.
[10] Mirza, A.N., Fornage, B.D., Sneige, N., Kuerer, H.M., Newman, L.A. & Ames, F.C. (2001). Radiofrequency ablation of solid tumors, pp. 95-102.
[11] Chang I. (2013). Finite element analysis of hepatic radiofrequency ablation probes using temperature-dependent electrical conductivity, Biomed Eng Online, pp. 2-12.
[12] Rhim, H., Goldberg, S.N., Dodd, G.D., Solbiati, L., Lim, K.L. Tonolini, M. & Cho, O.N. (2001). Helping the hepatic surgeon: Essential techniques for successful radio-frequency thermal ablation of malignant hepatic tumors, Radiographics, pp. 17-35.
[13] Kayssi, A., Pope, M., Vucemilo I. & Werneck, C. (2015). Endovenous radiofrequency ablation for the treatment of varicose veins, Can J Surg, pp. 85-86.
[14] Fisher, H.L. & Snyder, W.S. (1966). Annual progress report for Health Physics Division, Oak Ridge National Laboratory, Oak Ridge TN.
[15] Huang, H.W. (2015). Confluent Thermal Lesion Formation in Liver with Radio Frequency Ablation by Using Internally Cooled Multiple-Electrode Technique: Computational Results, Journal of Applied Science and Engineering, pp. 1-14.
[16] Jiang, Y. & Mulier, S. (2010). Formulation of 3D finite elements for hepatic radiofrequency ablation, Int. J. Modelling, Identification, and Control, pp. 1-13.
[17] Berjano, E.J. (20016). Theoretical modeling for radiofrequency ablation: state-of-the-art and challenges for the future, Biomed Eng Online, pp. 1-17.
[18] Shibeshi, S.S. & Collins, W.E. (2005). The rheology of blood flow in a branched arterial system, Applied Rheology, pp. 398–405.
[19] Liu, P., Liu, J. & Duan, H. (2012). Thermal modeling for endocardiac radiofrequency ablation: comparison bioheat equation and Pennes bioheat equation with the finite element, pp. 1-13.
[20] Weinbaum, S., Xu, L.X., Zhu, L. & Ekpene, A. (1997). A new fundamental bioheat equation for muscle tissue: part I—blood perfusion term, Journal of Biomechanical Eng., pp. 278–288.
[21] Mordon, S.R. Wassmer, B. & Zemmouri, J. (2006). Mathematical modeling of endovenous laser treatment (ELT), BioMedical Engineering Online, pp, 1-11.